Chapter 12 - **VELOCITY SELECTORS AND TIME-OF-FLIGHT MEASUREMENTS**

Characteristics of velocity selectors and time-of-flight measurement of the neutron wavelength distribution are described. Monochromation is a necessary step for SANS instruments that do not use the time-of-flight method. Continuous SANS instruments use velocity selectors instead of crystal monochromators. The basic concept for velocity selectors is to allow neutrons to travel in a rotating helical path. Neutrons that are either too fast or too slow get absorbed. Only neutrons with the right velocities are transmitted thereby transforming a white incident neutron spectral distribution into a monochromated distribution with mean wavelength λ and wavelength spread (FWHM) $\Delta\lambda$. Velocity selectors are either of the solid drum type (with helical slot) or of the multidisk type.

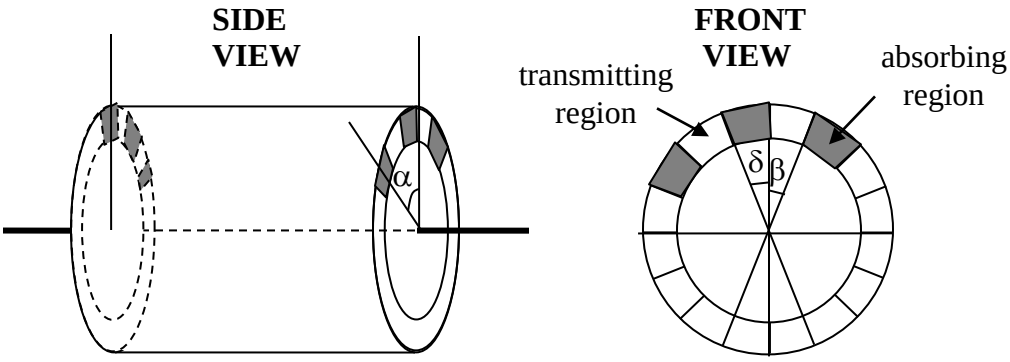

Figure 1: Schematics of a velocity selector explicitly showing three absorbing sectors and two transmitting windows between them.

1. VELOCITY SELECTORS CHARACTERISTICS

Velocity selectors rotate at constant frequency ω which is varied to change the transmitted neutron wavelength λ. A typical selector has an overall length L (length of the rotating "drum") and a radius R (between the selector rotation axis and the neutron window). The helical path is characterized by a pitch angle α. This is the angle by which the selector rotates while neutrons cross its length L.

Equating the time it takes for neutrons to travel that distance L to the time it takes the selector to rotate the angle α gives a relationship between the neutron wavelength λ and the rotation speed ω.

$$\lambda = \frac{\alpha h}{Lm\omega}. \qquad (1)$$

Here h is Planck's constant, and m is the neutron mass. This relationship is expressed in more convenient units as:

$$\lambda[\text{Å}] = 6.59 * 10^5 \frac{\alpha[\text{deg}]}{\omega[\text{rpm}]L[\text{mm}]}. \qquad (2)$$

Here, the selector rotation frequency ω is given in rpm (rotations per minute).

The selector transmission is proportional to the uncovered area of the input face. Two angles are defined. β is the angle subtending the transmitting window and δ is the angle corresponding to the absorbing region between two transmitting windows. The selector transmission is expressed as the following ratio:

$$T = \frac{\beta}{\beta + \delta}. \qquad (3)$$

The wavelength spread Δλ is defined as the FWHM of the selector output distribution. The selector resolution (relative wavelength spread) is simply expressed as the ratio of the two relevant angles.

$$\frac{\Delta\lambda}{\lambda} = \frac{\beta}{\alpha}. \qquad (4)$$

Note that $\Delta\lambda/\lambda$ is independent of λ so that the incoming λ^{-5} wavelength distribution from the neutron source becomes $\frac{1}{\lambda^4}\left(\frac{\Delta\lambda}{\lambda}\right)$ after the selector. Since $\Delta\lambda/\lambda$ is constant, this becomes a $1/\lambda^4$ distribution. The transmitted wavelength distribution is of the triangular form with slightly rounded angles (as will be described later).

To decrease the wavelength resolution, one can either (1) decrease the transmitting window angle β, or (2) increase the pitch angle α at the design stage. The first possibility is limited by the accompanying loss in selector neutron transmission. The second possibility comes with an increase in rotation speed in order to reach the same wavelength. In order to keep the same rotation speed, both the pitch angle α and the selector length L could be varied proportionately.

In order to change the wavelength spread of a selector, the selector axis is tilted (in the horizontal plane) by an angle ν relative to the beam axis thereby modifying the effective pitch angle as:

$$\alpha_{eff} = \alpha + \frac{\nu L}{R}. \qquad (5)$$

Tilting modifies both the wavelength spread $\Delta\lambda$ and the neutron wavelength λ.

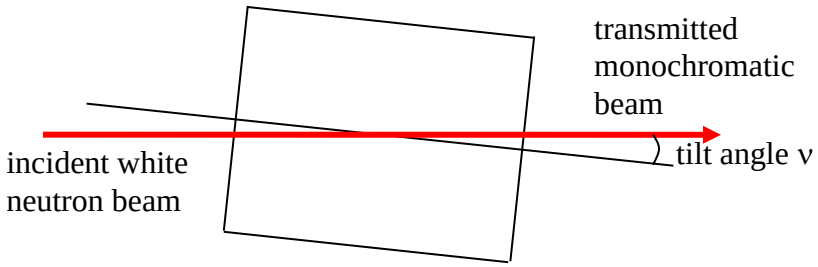

Figure 2: Schematic top view of a velocity selector showing the horizontal tilt angle ν.

2. TYPICAL VELOCITY SELECTOR

The following parameters correspond to a velocity selector used on a 30 m SANS instrument at the NIST Center for Neutron Research (Hammouda, 1992). It is a multi-disk unit of Hungarian type design.

Selector length L = 42 cm.
Radius to the middle of the window R = 17.5 cm.
Helix rotation angle $\alpha = 17^o$.
Open window aperture angle $\beta = 2.25^o$.
Absorbing region between windows $\delta = 0.75^o$.
Number of disks n = 22.

These design parameters yield the following predicted selector characteristics.

Neutron transmission T = 0.75.
Wavelength $\lambda[\text{Å}] = 2.669*10^4/\omega[\text{rpm}]$.
Relative wavelength spread $\Delta\lambda/\lambda = 0.132$ for a tilt angle of $\nu = 0$.
Effect of tilt angle ν on the helix angle $\alpha_{eff} = 17^o + 2.4\,\nu$.
Therefore $\left(\frac{\Delta\lambda}{\lambda}\right) = \frac{2.25^o}{17^o + 2.4\,\nu}$.

These are theoretical numbers predicted based on design parameters. Measured characteristics using the time-of-flight method are described in the following section.

3. VELOCITY SELECTOR CALIBRATION BY TIME-OF-FLIGHT

The time-of-flight (TOF) method consists in chopping the neutron beam (using a rotating chopper) and gating a neutron detector with the time-zero chopper pulse. All neutrons cross the chopper at the same time despite their spread in velocities. As neutrons travel beyond the chopper, they spread out with faster neutrons arriving to the detector first. The neutron pulse is sharp at the chopper level and becomes spread out at the detector level.

Here the time-of-flight method is used to characterize the wavelength distribution coming out of the velocity selector described earlier. The setup consists of a neutron disk-chopper followed by two pencil detectors installed close to the SANS instrument sample area. The pencil detectors have a diameter of 1.27 cm. The second pencil detector is used for redundancy and in order to obtain an exact measurement of the SANS sample-to-detector distance. The two pencil detectors are located 0.5 m apart and the distance between the second pencil detector and the area detector is 3 m. The chopper has a vertical neutron slit 1 mm wide and 1.27 cm tall. A fixed slit aperture of the same size is located just ahead of the chopper in order to define the neutron beam. The chopper rotation is synchronized with the neutron detectors data acquisition system through the time-zero pulse.

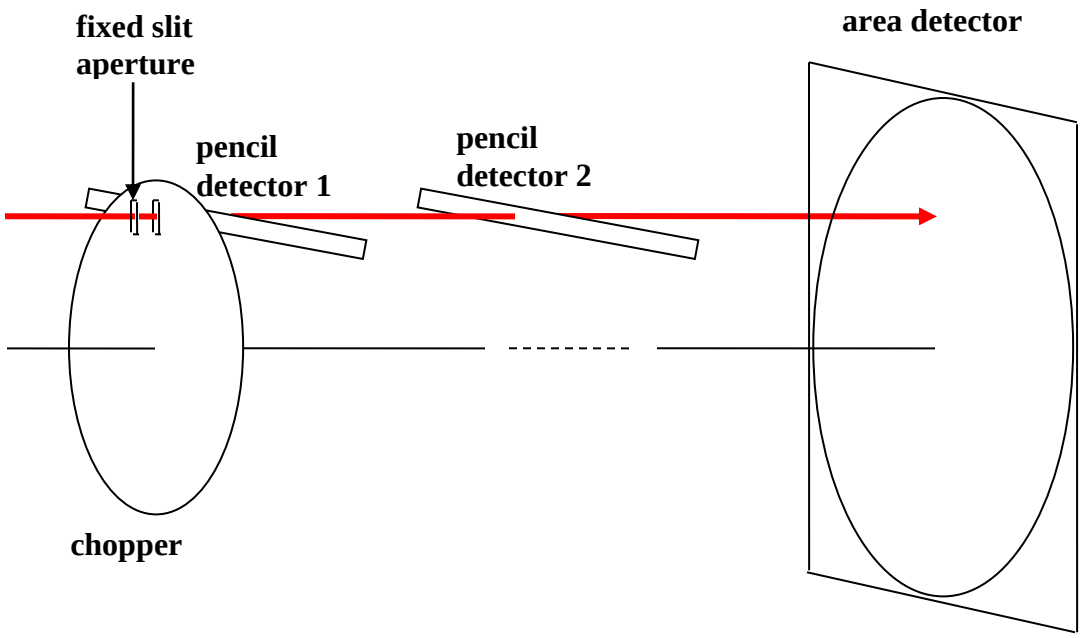

Figure 3: Schematic representation of the time-of-flight setup comprising a chopper, two pencil detectors and the area detector. The fixed slit aperture is located just before the chopper.

A multi-channel scaler electronic unit was used to record the neutron pulses from the neutron detectors using the gated signal from the chopper. A typical spectrum corresponding to a wavelength around 6 Å, a source-to-chopper distance of 14.27 m, a detector 1-to-detector 2 distance of 0.5 m and a pencil detector 2-to-area detector distance of 3 m is shown below.

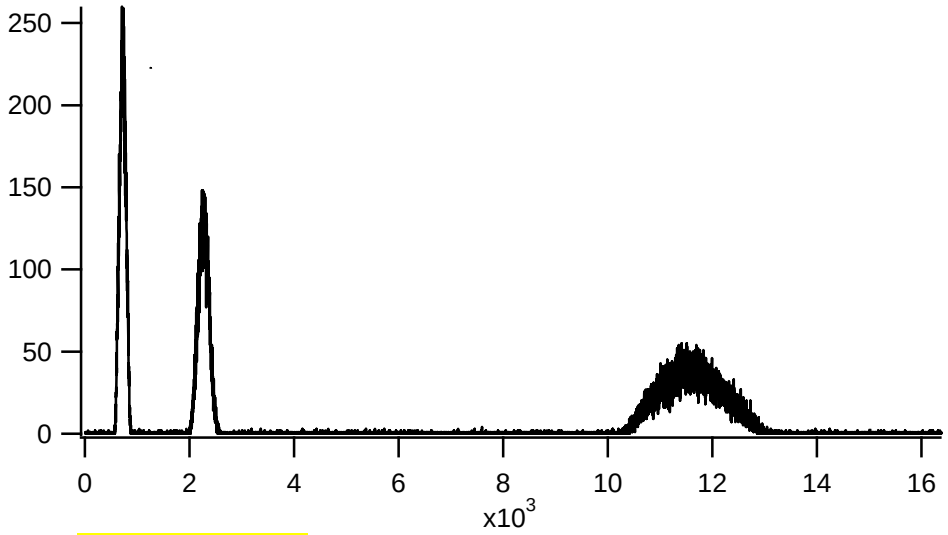

Figure 4: Neutron spectrum obtained by time-of-flight. The first two peaks were recorded by the two pencil detectors and the third peak was recorded by the SANS area detector. The horizontal axis is in time channel numbers (0.5 μsec/channel) and the vertical axis is in neutron counts. The chopper frequency was set to 113 Hz.

Fits of the various peaks to Gaussian shapes were performed in order to obtain peak positions and standard deviations. Peak positions yielded flight times (and therefore wavelengths) and standard deviations yielded wavelength spreads.

Wavelength Measurement

Knowing the distances between any two detectors, the neutron wavelength is proportional to the measured flight time between them and inversely proportional to the inter-distance between them.

$$\lambda[\text{Å}] = \frac{3.956 * 10^3}{v[\text{m/sec}]} \qquad (6)$$

v[m/sec] = inter-distance[m]/flight time[sec].

The velocity selector rotation speed was varied and the neutron wavelength was measured in each case. Using different detector pairs gave the same result.

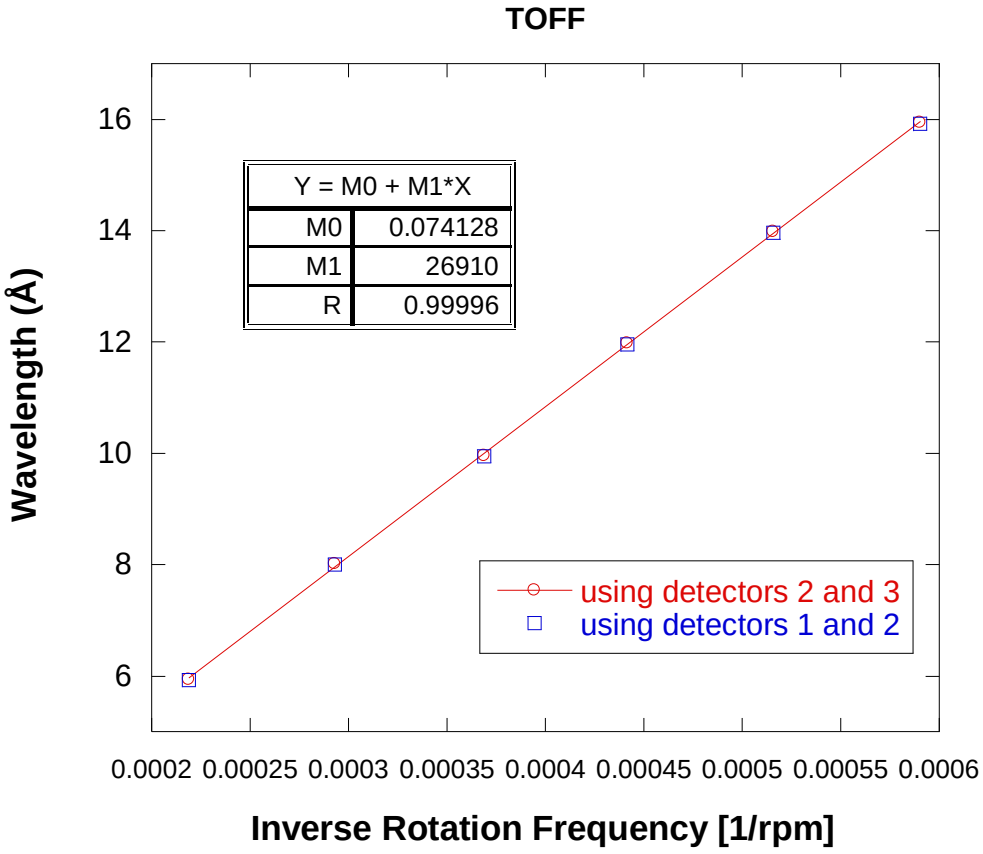

Figure 5: Variation of the measured wavelength with inverse velocity selector rotation frequency.

A linear fit to the λ[Å] with 1/ω[rpm] gives the following measured relationship:

$$\lambda[\text{Å}] = 0.0741 + 2.691 * 10^4/\omega[\text{rpm}]. \qquad (7)$$

The measured slope of $2.691*10^4$ agrees with the predicted one of $2.669*10^4$ reported earlier.

Variation of the neutron wavelength with inverse rotation frequency is plotted for three tilt angles.

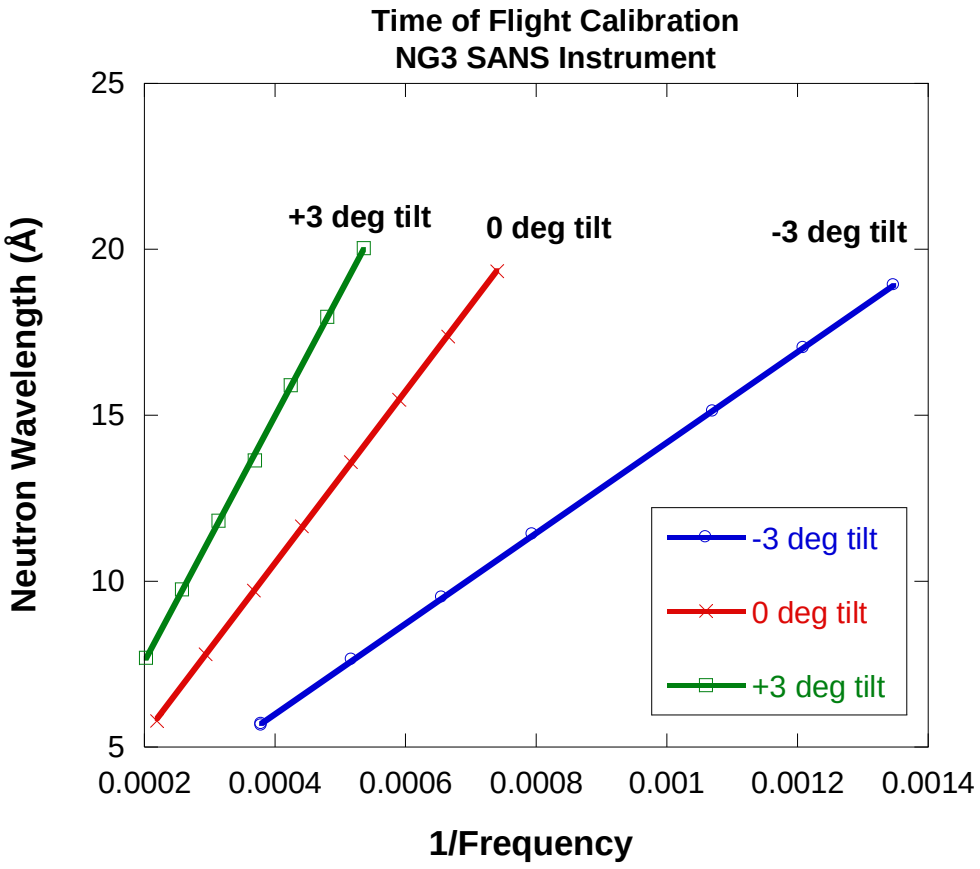

Figure 6: Variation of the measured wavelength with inverse frequency for three tilt angles.

Wavelength Spread Measurement

Gaussian fits to the measured spectra gave average flight times t_1, t_2 and t_3 and standard deviations σ_1, σ_2 and σ_3 for the peaks corresponding to detectors 1, 2 and 3 (recall that 1 and 2 are pencil detectors and 3 is the area detector). The relative wavelength spread obtained from detectors 1 and 3 is obtained as:

$$\left(\frac{\Delta\lambda}{\lambda}\right)_{1,3} = 2.355\frac{\sqrt{\sigma_3^{\,2}-\sigma_1^{\,2}}}{(t_3-t_1)}\sqrt{\frac{L_3-L_1}{L_3+L_1}}. \qquad (8)$$

Subtracting σ_1^2 insures that smearing contributions from the chopper's finite size slit (1 mm wide) and from the pencil detector's finite width (1.27 cm diameter) are removed. The factor $2.355 = 2(2\ln 2)^{1/2}$ is used to convert the standard deviation of the Gaussian shaped distribution σ into a full-width at half maximum (FWHM); $\Delta\lambda = 2(2\ln 2)^{1/2}\sigma_\lambda$.

The last term $\sqrt{\frac{L_3 - L_1}{L_3 + L_1}}$ is obtained through the following argument. The variance of the pulse time at a distance L_3 from the chopper is given by:

$$\sigma_t^2(L_3) = L_3^2\sigma_\tau^2 + \sigma_t^2(0). \qquad (9)$$

Here $\sigma_t(0)$ is the standard deviation at the chopper position and σ_τ is the standard deviation of the time-of-flight distribution. Applying this relation to two positions L_1 and L_3, one obtains the following relation:

$$\left(\frac{\sigma_\lambda}{\lambda}\right) = \left(\frac{\sigma_\tau}{\tau}\right) = \frac{\sqrt{\sigma_3^2 - \sigma_1^2}}{(t_3 - t_1)} \sqrt{\frac{L_3 - L_1}{L_3 + L_1}}\,. \qquad (10)$$

In practice $L_1 << L_3$ so that the last term (square root ratio) becomes unity.

Varying the velocity selector tilt angle decreases the relative wavelength spread.

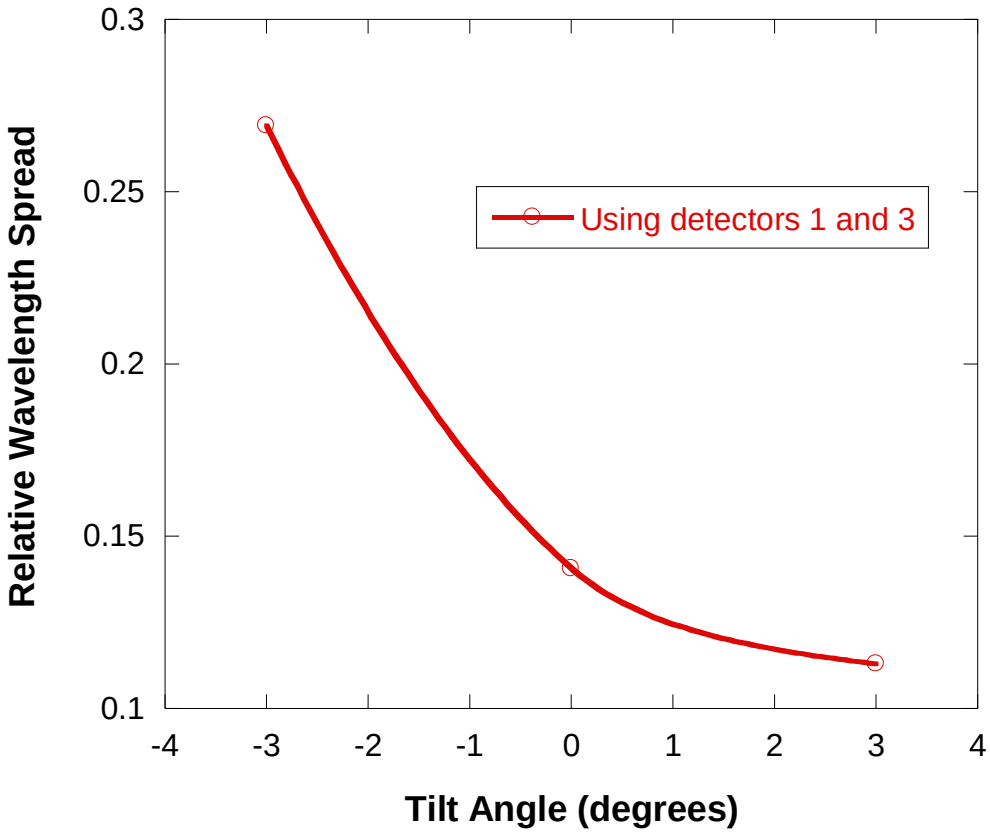

Figure 7: Variation of the measured relative wavelength spread with increasing selector tilt angle.

The measured relative wavelength spreads ($\Delta\lambda/\lambda$) corresponding to the three measured tilt angles (-3°, 0° and +3°) are 0.269, 0.141 and 0.113.

The measured inverse of the relative wavelength spread gives the following linear variation with the tilt angle ν.

$$\left(\frac{\lambda}{\Delta\lambda}\right) = 6.55 + 0.85\nu \ . \qquad (11)$$

This variation is far from the predicted value of

$$\left(\frac{\lambda}{\Delta\lambda}\right) = 7.55 + 1.07\nu \, . \qquad (12)$$

The wavelength spread is a very sensitive measurement to make. This is due to many factors: the assumption of Gaussian shape (for fitting purposes), smearing due to the defining slit's finite width, smearing due to the detectors finite detection depth, etc… For example, the pencil detectors are 1.27 cm in diameter and the area detector has a detection depth of 2.54 cm. Measured wavelength spreads are expected to be larger than predicted ones.

Wavelength Distribution Profile

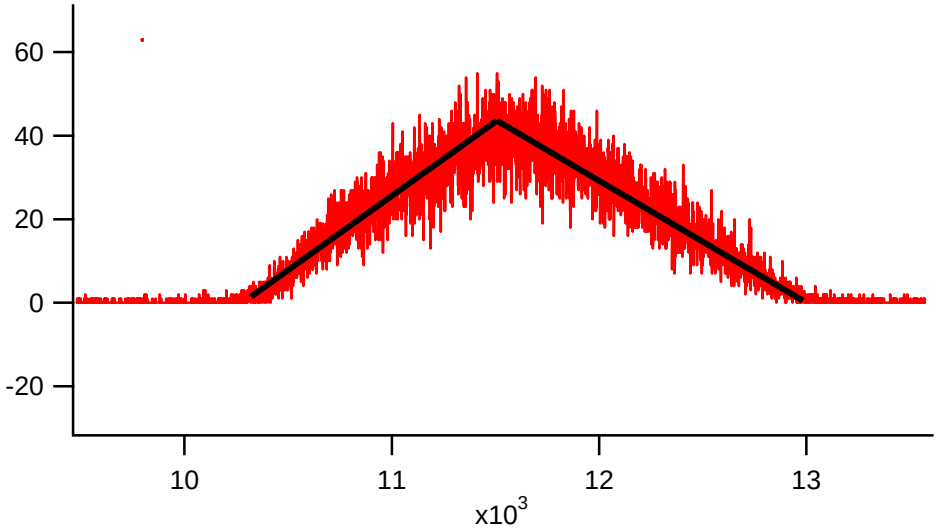

Figure 8: Wavelength distribution peak measured using the area detector with a wavelength around 6 A, a source-to-chopper distance of 14.27 m (corresponding to 1 pre-sample collimation guide inserted), and a pencil detector 2-to-area detector distance of 3 m. This distribution is characterized by a triangular shape.

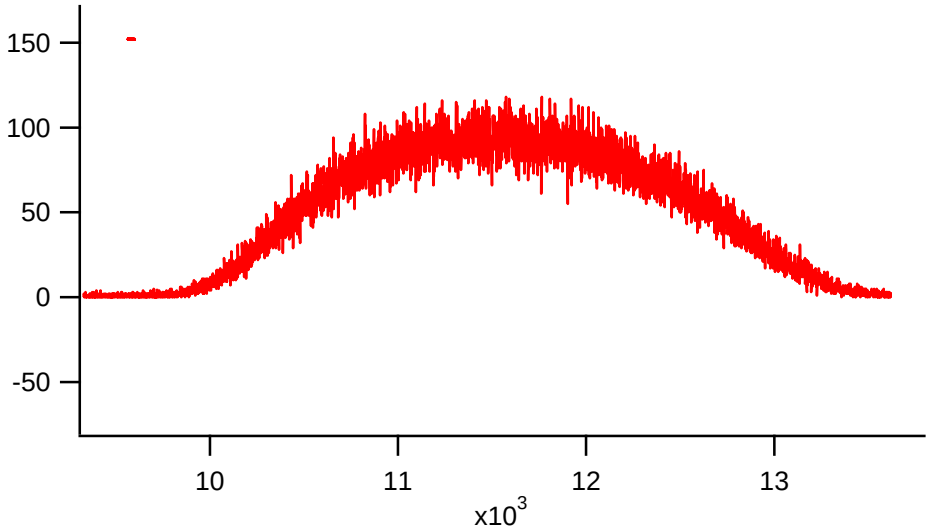

Figure 9: Wavelength distribution peak measured using the area detector with a wavelength around 6 A, a source-to-chopper distance of 3.38 m (corresponding to 8 pre-sample collimation guides inserted), and a pencil detector 2-to-area detector distance of 3 m. This distribution is characterized by a rounded Gaussian shape.

The source-to-chopper distance is varied by inserting neutron guides into the SANS instrument's pre-sample flight path. The monochromated neutron beam is therefore reflected (by the guides surface) before reaching the chopper. The first case shown corresponds to 1 guide inserted (source-to-chopper distance of 14.27 m) whereas the second case shown corresponds to 8 guides inserted (source-to-chopper distance of 3.42 m). The fist case is characterized by a triangular wavelength distribution whereas the second case is characterized by a rounded up Gaussian distribution (due to time-of-flight smearing). Inserted neutron guides introduce smearing to the wavelength distribution because they smear the flight time distribution.

Assuming a triangular wavelength distribution, the second moment is expressed as:

$$<\lambda^2>=<\lambda>^2\left[1+\frac{1}{6}\left(\frac{\Delta\lambda}{<\lambda>}\right)^2\right]. \qquad (13)$$

Assuming a Gaussian wavelength distribution, this quantity is expressed as:

$$<\lambda^2>=<\lambda>^2\left[1+\left(\frac{\sigma_\lambda}{<\lambda>}\right)^2\right]. \qquad (14)$$

Here σ_λ^2 is the variance of the Gaussian distribution defined as $\sigma_\lambda^2 = \langle\lambda^2\rangle - \langle\lambda\rangle^2$. Recall that the FWHM of a Gaussian distribution defined as $\Delta\lambda$ is given by $\Delta\lambda = 2(2\ln 2)^{1/2}\sigma_\lambda = 2.355\sigma_\lambda$. In this case:

$$\langle\lambda^2\rangle = \langle\lambda\rangle^2\left[1+\frac{1}{2.355^2}\left(\frac{\Delta\lambda}{\langle\lambda\rangle}\right)^2\right]. \qquad (15)$$

In order to simplify the notation, $(\Delta\lambda/\langle\lambda\rangle)$ is often represented by $(\Delta\lambda/\lambda)$.

Discussion

Wavelength calibration can be performed by either measuring a sample with a well-defined SANS peak or by the time-of flight method. The measured neutron wavelength agrees with prediction whereas it is hard to precisely predict the wavelength spread. Many time-smearing (or pulse-broadening) factors contribute to the uncertainty in wavelength spread. For example, increasing the chopper frequency decreases this time smearing. Time-of-flight calibration measurements are better performed with a high chopper frequency even if peaks corresponding to consecutive time frames overlap. It is easier to unravel what peak corresponds to what time frame than introduce a systematic uncertainty due to changing chopper frequency.

The finite depth of the detector volume in area detectors introduces more pulse broadening. Moreover, increasing the neutron wavelength decreases the sample-to-detector distance measurably (by as much as 1.27 cm equivalent to the active depth up to the anode plane in the area detector) because slower neutrons are stopped closer to the entrance side of the detection volume. This is due to the "1/v"-dependence of the neutron absorption cross-section in He-3.

Inserting neutron guides between the velocity selector and the sample (done to reduce the SANS source-to-sample distance) rounds off the edges of the neutron spectral distribution from a triangular shape to a Gaussian shape. This increases the wavelength spread.

Such "second order effect" corrections could include (1) slight variation of the wavelength spread with wavelength and with number of guides in the incident pre-sample flight path collimation, and (2) slight variation of the sample-to-detector distance with wavelength.

Some of the issues discussed here are essential in understanding the resolution of time-of-flight (TOF) SANS instruments located at pulsed neutron sources.

The Graphite Bragg Diffraction Edge

In order to independently check the wavelength calibration, it is nice to use other methods. The Bragg edge method is reliable. The Bragg law $\lambda = 2d \sin(\theta/2)$ relates the neutron wavelength λ, the d-spacing of a crystal d, and the scattering angle θ. The Bragg edge occurs when the incident neutrons are parallel to the crystal lattice planes. This is obtained when $\theta/2 = 0^o$ or 180^o. There is a drop in diffraction intensity at that condition (neutrons are transmitted through rather than diffracted). Note that the scattering angle is defined as θ in SANS terminology (not as 2θ as done in some diffraction books).

Polycrystalline graphite is characterized by a Bragg diffraction edge at 6.708 Å. Placing a graphite block in the neutron beam along with the time-of-flight setup gives an independent check of the wavelength calibration. A pencil detector and the area detector are used in the time-of-flight setup. The spectrum shown in the figure corresponds to a neutron wavelength around 6.7 Å, a source-to-chopper distance of 5.42 m, and a pencil detector-to-area detector distance of 6 m. Here only one pencil detector and the area detector are used. A chopper frequency of 70 Hz and a dwell time of 1 μsec were used. The first sharp peak corresponds to the pencil detector located just after the chopper. The broad peak corresponds to the area detector and shows the graphite edge. The second narrow peak corresponds to the next neutron pulse on the pencil detector.

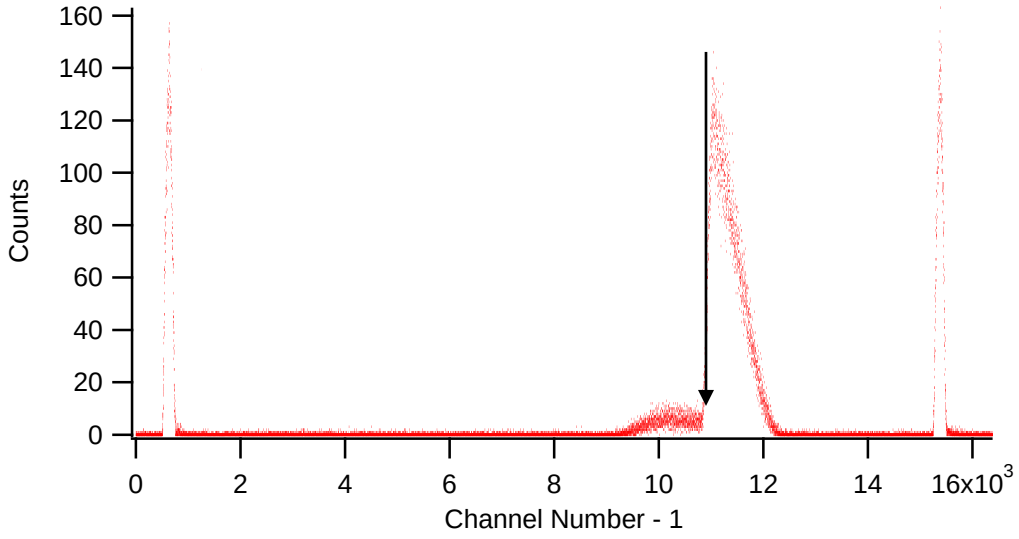

Figure 10: Time-of flight spectrum using a pencil detector and the area detector and placing a (4 cm thick) polycrystalline graphite block just after the pencil detector. Graphite is characterized by a sharp Bragg diffraction edge at 6.708 Å (located by the arrow).

4. OTHER WAVELENGTH CALIBRATION METHODS

There are other methods to calibrate the neutron wavelength based mostly on scattering samples that are characterized by Bragg peaks in the SANS range. Here Silver Behenate and Kangaroo tail tendon are discussed briefly.

Silver Behenate

Silver Behenate is characterized by a sharp Bragg ring with a d-spacing of 58.38 Å. It is useful for a "quick" wavelength check. It cannot, however, be used to determine the wavelength spread.

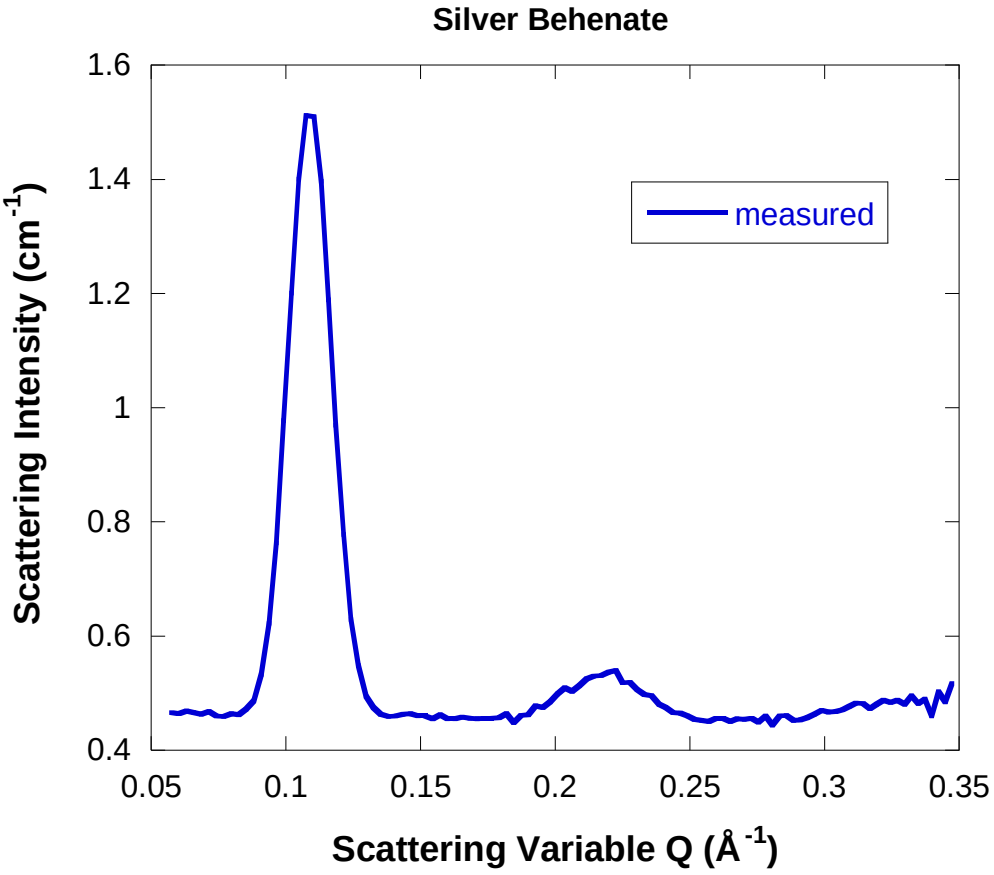

Figure 11: SANS spectrum from Silver Behenate showing a sharp first peak at Q = 0.1076 $Å^{-1}$ (d-spacing of 58.38 Å).

Kangaroo Tail Tendon

Kangaroo tail tendon is characterized by a regular periodic structure along the fiber with a d-spacing of 667 Å. SANS scattering from Kangaroo tail tendon in D_2O is anisotropic. Sector averaging along the Bragg spots shows many order reflections. The first peak is

strong, the second reflection is extinct and the third peak is well defined even with typical SANS smearing ($\Delta\lambda/\lambda = 0.13$).

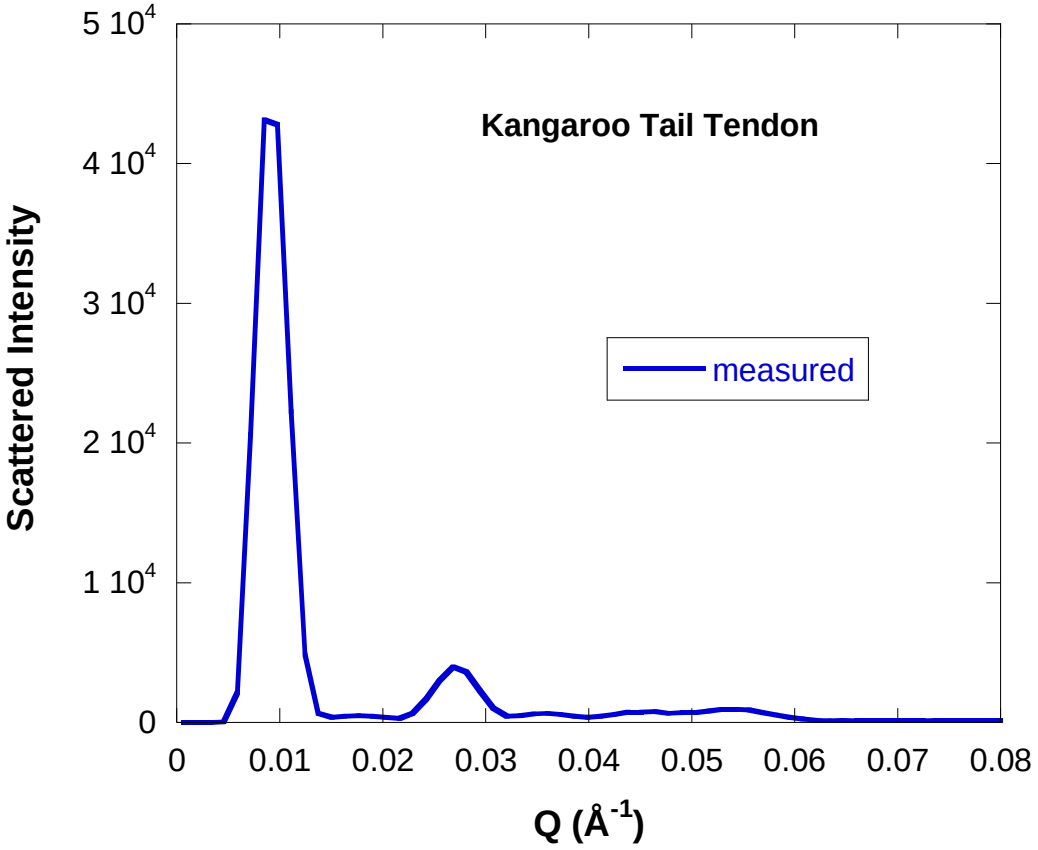

Figure 12: SANS spectrum from Kangaroo tail tendon characterized by a first sharp peak at Q = 0.00942 $Å^{-1}$ corresponding to a d-spacing of 667 Å. The third order peak is also strong.

5. DISCUSSION

Monochromation is an essential step for SANS as well as other diffraction methods. Instruments located at pulsed neutron sources use the time-of-flight method. Continuous beam instruments use either velocity selectors or crystal monochromators. Velocity selectors are preferred because monochromation occurs without change in the incident beam direction. When using crystal monochromators, the entire SANS instrument has to be rotated horizontally around the crystal monochromator axis in order to change neutron wavelength. This is a prohibiting factor in guide halls where experimental space between close together guides is at a premium. An advantage of crystal monochromators is the tight wavelength spread due to the typically small mosaic spread of crystals. That spread can be widened by using superlayers of slightly misaligned crystals. Velocity selectors commonly cover a wide wavelength spread (from $\Delta\lambda/\lambda = 10$ % to 30 %). Crystal monochromations cover the lower scale (from $\Delta\lambda/\lambda = 0.1$ % to 5 %). The use of two

velocity selectors in parallel (for either low or wide $\Delta\lambda/\lambda$) would be a nice option for both low-resolution and high-resolution SANS measurements.

REFERENCE

L. Rosta, "Multi-Disk Neutron Velocity Selectors", Physica B156-157, 615-618 (1989).

B. Hammouda, "Multidisk Neutron Velocity Selectors", Nuclear Instruments and Methods in Physics Research A321, 275-283 (1992).

QUESTIONS

1. How does a velocity selector work?
2. How does a crystal monochromator work?
3. What is the main characteristic of a SANS instrument that uses a crystal monochromator?
4. Does the velocity selector transmission vary with neutron wavelength?
5. Does the predicted relative wavelength spread vary with neutron wavelength?
6. What is the wavelength dependence of the neutron spectrum before and after the velocity selector?
7. What is the purpose of tilting a velocity selector to an angle with respect to the neutron beam? What is the range of effective tilt angles?
8. How would you measure the transmission of a velocity selector?
9. What are the main pieces of equipment necessary to perform time-of-flight measurements?
10. What samples are characterized by sharp peaks in the SANS range and could be used for cold neutron wavelength calibration?
11. The standard deviation of a Gaussian distribution σ can be related to its full-width at half maximum (FWHM) by $FWHM = 2(2\ln 2)^{1/2}\sigma$. Derive this factor.
12. Velocity selectors transform the neutron wavelength distribution from Maxwellian tail to a triangular distribution. Why is that?
13. Assuming a triangular wavelength distribution outputted by a velocity selector calculate the variance $\sigma_\lambda^2 = \langle\lambda^2\rangle - \langle\lambda\rangle^2$.
14. What causes a Bragg diffraction edge? Bragg diffraction edges occur at what wavelengths for graphite and for beryllium?
15. Find out possible suppliers of velocity selectors. What are the essential characteristics to provide to a potential supplier.
16. Find out possible suppliers of neutron choppers, pencil detectors and multi-channel scalers.

ANSWERS

1. A velocity selector works by letting through only neutrons of the right speed.

2. A crystal monochromator uses the Bragg law of diffraction. It works by scattering neutrons of a certain wavelength into a specific scattering angle.
3. A SANS instrument that uses a crystal monochromator has to pivot around the vertical monochromator axis in order to change the neutron wavelength.
4. The predicted velocity selector transmission does not vary with wavelength.
5. The predicted relative wavelength spread does not vary with wavelength.
6. The tail of the Maxwellian neutron spectrum from the cold source varies like $1/\lambda^5$ whereas after the velocity selector the spectrum varies like $1/\lambda^4$ where λ is the neutron wavelength.
7. Velocity selectors are tilted horizontally in order to vary the wavelength spread. Tilt angles vary between -3 ^{o} to +3 ^{o}.
8. The transmission of a velocity selector could be measured similarly to the transmission of any SANS sample, by using a second selector operating at the same wavelength at the sample location. Transmission is the ratio of the detector counts with the selector in over that with the selector out (i.e., removed).
9. Time-of-flight measurements can be performed using a chopper, two detectors positioned a known distance apart and a multi-channel scaler gated with the time zero from the chopper.
10. Examples of samples that are characterized by sharp peaks in the SANS range include: Silver Behenate, phase separated copolymers, fibers like collagen from a Kangaroo tail tendon, highly packed silica or latex particles.
11. Consider a Gaussian function $P(\lambda) = (1/2\pi\sigma^2)^{1/2} \exp(-\lambda^2/2\sigma^2)$ where σ is the standard deviation. Setting $P(\lambda) = ½$, two solutions can be found for $\lambda = \pm \sqrt{2\ln(2)}\,\sigma$. This yields a band FWHM = $\Delta\lambda = 2\sqrt{2\ln(2)}\,\sigma = 2.355\sigma$.
12. The output of a velocity selector is a triangular wavelength distribution because of the geometry of neutron trajectories through the selector windows.
13. Consider an isosceles triangular distribution of FWHM $\Delta\lambda$ (and base $2\Delta\lambda$) and centered at a wavelength λ_0. The left side of the triangle is given by $F(\lambda) = (\lambda-\lambda_0)/\Delta\lambda + 1$. The right side of the triangle is given by $F(\lambda) = (-\lambda+\lambda_0)/\Delta\lambda + 1$. The variance $\sigma_\lambda^2 = \langle\lambda^2\rangle - \langle\lambda\rangle^2$ involves the following integrations $\sigma_\lambda^2 = \langle\lambda^2\rangle - \langle\lambda\rangle^2 =$

$$\frac{\int_{\lambda_0-\Delta\lambda}^{\lambda_0} d\lambda\lambda^2\left(\frac{\lambda-\lambda_0}{\Delta\lambda}+1\right) + \int_{\lambda_0-\Delta\lambda}^{\lambda_0} d\lambda\lambda^2\left(\frac{-\lambda+\lambda_0}{\Delta\lambda}+1\right)}{\Delta\lambda} = \frac{1}{6}(\Delta\lambda)^2 .$$

14. A Bragg diffraction edge occurs when the incident neutrons are parallel to the crystal lattice planes and the crystal is probed edgewise. Bragg diffraction edges for graphite and beryllium occur at neutron wavelengths of 6.708 Å and 4.05 Å respectively.
15. Possible suppers of velocity selectors are the KFKI Hungarian and the Dornier German companies.
16. There are many suppliers of choppers and a wide range in prices. For multi-channel scaler suppliers, the name Ortec comes to mind. Neutron pencil detectors are sold by Reuter Stokes and by Lehnard Neutron Detector (LND). Both are companies based in the USA.